



Contents lists available at ScienceDirect

## Sensors and Actuators A: Physical

journal homepage: [www.elsevier.com/locate/sna](http://www.elsevier.com/locate/sna)



# Wearable inertial mouse for children with physical and cognitive impairments

R. Raya\*, J.O. Roa, E. Rocon, R. Ceres, J.L. Pons

Instituto de Automática Industrial, CSIC, Ctra. Campo Real km. 0.200, 28500 Arganda del Rey, Spain

### ARTICLE INFO

#### Article history:

Received 30 September 2009  
Received in revised form 10 March 2010  
Accepted 12 April 2010  
Available online xxx

#### Keywords:

Inertial sensors  
Human machine interface  
Cerebral palsy  
Assistive technology  
Wearable

### ABSTRACT

People with multiple physical and cognitive impairments have difficulties for using properly conventional pointing devices, what reduces their possibilities to communicate and improve their cognitive and physical skills through computers. This paper proposes a head control mouse based on a triaxial inertial sensor particularly focused on infants with cerebral palsy (CP). The system consists of a real-time head tracker that translates the head orientation into pointer positions and measures kinematic parameters through the 3D inertial sensor. The algorithm to estimate the angular head orientation is presented and validated with an accuracy about 1°. The experimental results with five healthy users demonstrated that the inertial pointer succeeds what was validated according to the ISO 9241-Part9. The experimental results with two infants with CP (athetoid and dystonic cases) demonstrated that the infants are capable of placing the pointer around the target but they have difficulties for fine motor control. The inertial sensor offers interesting kinematic parameters of the pathological movement. These parameters can be directly obtained by the inertial signals and are very useful to design filtering techniques to extract voluntary intentions. A research technique for filtering some patterns of the involuntary movements is presented. The inertial interface constructed and validated in this paper will allow increasing the knowledge about the pathological motion of the infants with CP.

© 2010 Elsevier B.V. All rights reserved.

## 1. Introduction

Our global society is increasingly taking into account the challenges disabled people encounter on a daily basis. The importance of this can be observed both in the large number of affected people and the limited opportunities for social, professional, and personal reintegration and advancement. Currently, an estimated 10% of the world's population experiences some form of disability or impairment [37]. The number of people with disabilities is increasing due to population growth, ageing, emergence of chronic diseases and medical advances that preserve and prolong life. Both physical and cognitive disabilities affect to motor skills and social integration. Severe neuromotor disorders are often accompanied by mental deficit. This is particularly true for children affected by cerebral palsy (CP).

CP is the most common cause of disability affecting the functional development of children. The most frequently cited definition of CP is a *disorder of posture and movement due to a defect or lesion in the immature brain* [3]. The prevalence of CP is internationally 1.5–2.0 cases per 1000 births. Only in the United States 500,000 infants are affected by CP [51]. In Europe these figures are

even higher [22]. Treatments for CP patients depend on the specific patients' pathology and range from physical therapy to medication and surgery. When distinguishing therapeutic approaches on their main emphasis, the following basic principles can be recognized: (1) emphasis on normalization of the quality of movement [23]; and (2) emphasis on functional activities, which focuses on the development of skills necessary for the performance of activities of daily living [24]. Approximately 50% of children affected by CP need technical aids for assisting their mobility (braces, walkers, or wheelchairs). In addition, 70% of them exhibit other disabilities [10].

It is demonstrated that it is during early stages of development that fundamental abilities and skills are developed [18,20]. Thus, it is crucial to give infants an opportunity to interact with the environment for an integral development. It is recognized that assistive technology can improve the functional capabilities limited by CP [25,52]. Concretely, the interaction between the infant and the computer is considered an interesting way for empowering the residual capabilities [31,1]. For instance, video games increase the efficiency of information processing and concentration skills among learning [28]. The computer allows infants to learn through the interaction with virtual environments providing new opportunities for communicating and new therapies. With these virtual environments, the conditions of the therapy, such as time or intensity of the task can be easily configured by clinical professionals. However, the conventional human computer interfaces

\* Corresponding author. Tel.: +34 91 8711900; fax: +34 91 8717050.  
E-mail address: [rraya@iai.csic.es](mailto:rraya@iai.csic.es) (R. Raya).  
URL: <http://www.iai.csic.es> (R. Raya).

such as mouses, keyboards or joysticks, are difficult to control for people with cognitive and physical impairments, thus diminishing the opportunities to access to the computer. Physical disabilities, particularly the CP, limit the motor control. Due to these limitations, numerous research groups are working to find interfaces focused on restoring and augmenting the human capabilities.

Many researches on assistive technology are focused on designing hands-free interfaces. Interfaces that use switches to control a computer have been used for a considerable period and are still popular [47]. Some of them used the residual capabilities as breath expulsion [9,33], switches contacted by operator's cheek [11], tongue movements or mouthsticks [36]. Nowadays, new technologies are giving place to advanced and bio-inspired interfaces which augment these residual capabilities [13,6]. Over the last decade, active researches have proposed a wide variety of mouse replacement interfaces with the movement of eyes, nose, and face [49,5,43,32]. The most current designs are video-based with webcams [30] or infrared sensors [8]. Eye and gaze-based interfaces have the potential to be a very natural form of pointing, as people tend to look at the object they wish to interact with. Moreover, they do not require the user to wear anything in contact with the body. In these approaches the system can track either the movement of the head, or the pupil's movement relative to the head. In the last case, the user's head must remain fixed in relation to the camera position. Another approaches require infrared emitters that are attached to the user's forehead or on a pair of glasses. This approach reduces significantly the high processing overheads of the video-based approach. Other interfaces use infrared light emitting diodes (LED's) and photodetectors to determine head position [16].

Other approaches do not use video images but detect user intentions by measuring the corneal-retina activity (electrooculography, EOG) [14] or through biological signals such as electroencephalographic activity (EEG [39,38]) or muscular activity (electromyography, EMG [40]). Some approaches use a combination of different technologies as the EMG signals from muscles in the face and point of gaze coordinates produced by an eye-gaze tracking system [12]. Some devices are voice-based human computer interfaces in which a set of commands can be executed by the voice of the user [7,19]. Since many individuals with motor impairments have complete use of their vocal system, these devices make use of it. However, standard spoken language are useful and natural for communication between humans but not so natural between human and computer.

Some interfaces combine vision and inertial sensors to track the movements of some human body parts [48]. Most of the approaches used in 3D inertial input devices are based on the measurement of the angular velocity with gyroscopes and the measurement of linear acceleration with accelerometers [15]. Due to recent development in micro-machining technology, the cost of micro-machined accelerometer is decreasing while the accuracy is being improved. Also, less fundamental physical constraints inhibit the precision of micro-machined accelerometer than that of gyroscope [42]. There are some head operated computer mouse that employs tilt sensors placed in a headset [11]. Other interfaces integrate three dimensional accelerometer, gyroscope and magnetometer to reach a higher precision [35]. In many cases, the inertial sensors are used for rehabilitation because these sensors represent a real scientific breakthrough in the medical field, where there is a need for measuring the kinematics of body segments [44].

Although there are many developments for disabled people in general, there are few evidences from motor disabled community using these alternative interfaces [2]. The inertial interface presented by this paper is addressed to people with pathological movements, which involve voluntary and involuntary movements, such as tremor or spasms. Thus, the intended interface must integrate some techniques to filter these undesired movements and

detect the voluntary intentions. These filtering techniques will be based on kinematic parameters, such as motion frequency, acceleration or angular velocity. These parameters can be obtained directly using the signals of the inertial sensor for each axis independently. However, other interfaces such as eye or face-based tracking, need more complex algorithm (image processing and 3D modelling) to obtain these kinematic parameters [41,8]. Inferring 3D scene properties from 2D image measurements is an underconstrained task due to the lack of depth information [48]. Moreover, although video-based interfaces do not require to wear anything, the user must focus on the cursor's movement on the computer screen and assure that the transmitted signals are within the reception range of the receiver. As a result, these devices certainly cause troubles for people with involuntary movements such as tremor or spasms. According to these considerations, the authors consider that the inertial technology is the most efficient for human motion analysis and especially for the pathological motion assessment. Although all areas of the motor function are limited, limbs are usually more affected than the head motion in infants with CP [50]. Hence, the inertial interface presented by this paper is a head mounted device.

Section 2 of this paper summarizes the technical specifications of the inertial sensor (IMU). Section 3 describes the process to convert the head's motion to mouse pointer positioning. The algorithm to calculate the angular orientation of the IMU is presented by Section 3.1. The algorithm to translate the angular orientation to pointer coordinates is described by Section 3.2. Section 3.3 describes the validation of the angular orientation of the IMU using a photogrammetric system as an absolute reference. Section 4 collects the results of two types of experiments: (1) the tests performed by five healthy participants to validate the inertial interface, (2) and the tests performed by two infants with CP. Finally, Section 5 some interesting considerations, conclusions and future work are exposed.

## 2. The inertial unit

The interface consists of a headset with a commercial helmet and an inertial measurement unit (IMU, Fig. 1). The IMU (developed by the collaboration between the authors and Technaid S.L.) integrates a three-axis gyroscope, accelerometer and magnetometer. A rate gyroscope measures angular velocity by measuring capacitance and it is based on the Coriolis force principle during angular rate. The accelerometer measures the gravity and the acceleration caused by motions (by Hookes law). The magnetometer measures the earth magnetic field. The 3D IMU is based on MEMS technology and is available in a package measuring 27 mm × 35 mm × 13 mm and its weight is 27 g which is less than other sensors used in the field [45,34,46]. The 3D IMU is capable of sensing ±2.0 Gauss, ±500°/s angular rate and ±3 g acceleration about three axes independently. It has an angular resolution of 0.05°, a static accuracy less than 1° and a dynamic accuracy about 2° RMS. The 3D IMU provides digital outputs.

## 3. The algorithm for pointer control

### 3.1. Angular orientation of the inertial measurement unit

The algorithm aims to translate the head's motion into the corresponding mouse pointer positions. As IMU is attached to the user's head, the angular orientation of the IMU is the angular orientation of the head. Therefore, the first step is to estimate the angular orientation of the IMU.

First of all, the digital signals of the IMU have to be converted to physical outputs by a calibration process. The IMU calibration protocol consists of six static positions and three rotations which are



Fig. 1. Trials with the inertial interface (left). The inertial interface (right). The communication between the interface and the computer can be USB or Bluetooth.

summarized in Table 1. The IMU digital signals (from magnetometers, gyroscopes and accelerometers) in XYZ frame were recorded during selected period of time for each static position. Since the calibration process is done with a sample rate of 50 Hz, 10 s was enough to get the sufficient amount of samples that are needed in calibration process. Rotations of 90° were used in the calibration process. Following the procedure proposed by Ferraris et al. [17], the recorded signals are used to calculate: The nonlinearity among 9 IMU sensors and the box where they are placed, the bias, and the scale factor of signals. Then, the calibration information is used to adjust the IMU physical outputs in the real time process. Fig. 3 shows the pseudo-code of the whole process. This part corresponds to the instructions called “Calibration process”.

The algorithm uses the 3D accelerometer as an inclinometer and the 3D magnetometer as a compass. Accelerometer’s signals contain accelerations caused by motion and gravity. To use the accelerometer as inclinometer is necessary to remove the accelerations caused by motion. They can be removed by filtering the acceleration with a low pass IIR filter (with first-order in the feed-forward loop and third-order in the feedback loop). The filter has been calculated according to a characterization of human motion in which it is demonstrated that the average predominant frequency component of the daily living activities is about 1 Hz with 75% of the spectral energy < 5 Hz [29]. The IIR filter designed does not have any ripple in the pass band range. Filters such as Chebychev-I and elliptical introduce ripple in the passband, while the Chebychev-II exhibits ripple in the stopband. It was chosen a Butterworth filter because is ripple-free and it has a quasi-linear response in the pass-band. Fig. 2 depicts the response and the transfer function (in the z-transform domain) of the designed filter (see Fig. 3, ‘Low-pass filter’). The complete transfer function is:

$$Y(z) = \frac{0.1}{1 - 0.63z^{-1} - 0.18z^{-2} - 0.09z^{-3}} \quad (1)$$

Once digital outputs have been converted to physical outputs and the IIR filter has been applied, the sensory information is fused

Table 1  
Positions and rotations used in the calibration process of the IMU.

| Type       | Description  |
|------------|--|
| Position 1 | $\vec{X}$ parallel to the gravity, $\vec{Z}$ parallel to the magnetic north.     |
| Position 2 | $\vec{X}$ antiparallel to the gravity, $\vec{Z}$ parallel to the magnetic north. |
| Position 3 | $\vec{Y}$ parallel to the gravity, $\vec{X}$ parallel to the magnetic north.     |
| Position 4 | $\vec{Y}$ antiparallel to the gravity, $\vec{X}$ parallel to the magnetic north. |
| Position 5 | $\vec{Z}$ parallel to the gravity, $\vec{Y}$ parallel to the magnetic north.     |
| Position 6 | $\vec{Z}$ antiparallel to the gravity, $\vec{Y}$ parallel to the magnetic north. |
| Rotation 1 | Rotation of a known angle around $\vec{X}$                                       |
| Rotation 2 | Rotation of a known angle around $\vec{Y}$                                       |
| Rotation 3 | Rotation of a known angle around $\vec{Z}$                                       |

to calculate the angular orientation of the IMU. First of all, using the 3D magnetometer signals is created an unit vector called  $\vec{H}$  and using the 3D accelerometer signals is created an unit vector called  $\vec{Z}$ . The cross product of  $\vec{H}$  and  $\vec{Z}$  gives a perpendicular vector called  $\vec{Y}$ . The cross product of  $\vec{Y}$  and  $\vec{Z}$  gives the vector  $\vec{X}$ . The orientation matrix is formed by the vectors  $\vec{X}$ ,  $\vec{Y}$  and  $\vec{Z}$  which are the orientation coordinates of the inertial unit housing in the sensor frame at each step ( ${}^sR_s = [{}^s\vec{X}_s {}^s\vec{Y}_s {}^s\vec{Z}_s]$ , see graphic 3, ‘Get Orientation IMU’). The validation of the algorithm is described by Section 3.3.

The 3D gyroscope is not used to calculate the angular orientation. The gyroscope used presents a slow variable offset with the temperature. Hence, if angular rotation is calculated by integrating the gyroscope signals, it will be necessary to subtracted this offset to avoid a systematic bias [26]. Hence, it would introduce unnecessary complexity for the algorithm. However, the 3D gyroscope signals are interesting for the pathological characterization because the angular velocity is an important kinematic parameter.

### 3.2. Correspondence between head orientation and pointer position

The movements used to locate the pointer on the screen are yaw and pitch (see Fig. 4). The Yaw motion corresponds to horizontal displacement of the pointer and Pitch motion corresponds to vertical displacements of the pointer. At the beginning, the angular ranges (horizontal,  $\theta_h$  and vertical  $\theta_v$ ) of the head’s motion has to be calculated by means of a calibration method. The calibration method consists of looking at two points of the screen (left/up (A) and center (B), see Fig. 4) and the ranges are automatically calculated. The ranges can be also manually introduced by the clinical professionals, because of many infants have problems to control the head in a specific position during a certain amount of time. The angular orientation at the point B is called  ${}^GR ([{}^G\vec{X} {}^G\vec{Y} {}^G\vec{Z}]$ ). It is the absolute reference frame which define the planes  $\Pi_1$  and  $\Pi_2$ . The horizontal and vertical coordinates of the pointer are called  $x$  and  $y$  respectively. The corresponding pointer coordinates to the absolute reference frame  ${}^GR$  are the coordinates of the screen center which are called  $x_c$  and  $y_c$ .

The pointer is located by absolute positioning because a concrete angular orientation always corresponds to the same pointer coordinates. Fig. 5 depicts how the angular orientation of the head is translated to pointer coordinates (horizontal in the left side, and vertical in the right side). The process is based on the axis  $\vec{X}$  because this vector is like a virtual stick attached to the user’s forehead (see Fig. 4). First of all, the angular orientation in the sensor frame,  ${}^sR_s$ , is referenced to the absolute reference frame as  ${}^GR_s = {}^GR \cdot {}^sR_s = [{}^G\vec{X}_s {}^G\vec{Y}_s {}^G\vec{Z}_s]$  at each step. Secondly, the vector  ${}^G\vec{X}_s$  is geometric projected onto the horizontal plane  $\Pi_1$  giving place to the 2D vector called  ${}^G\vec{X}_s \mathbf{P} \llbracket \cdot \rrbracket_1$ . The projection of this 2D vector on the

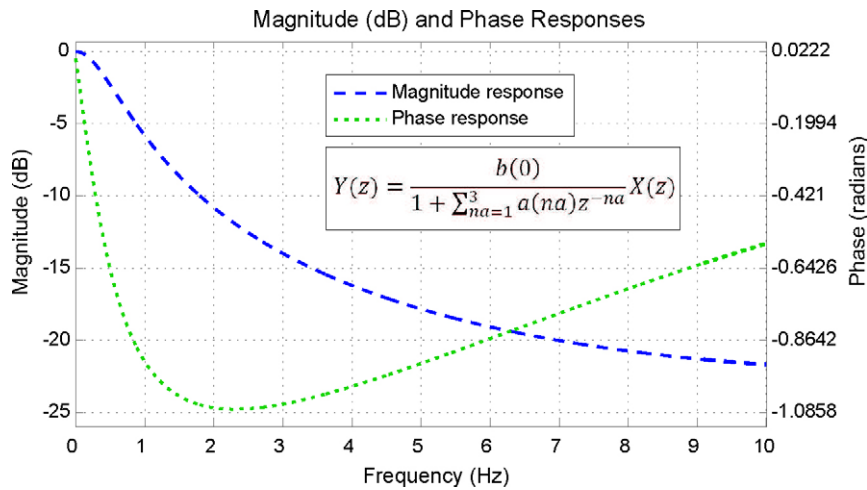


Fig. 2. Magnitude and phase response and transfer function of the IIR filter.

### Positioning Cursor Algorithm

**Date:**  ${}^G R \in R_{3 \times 3}$ , Global reference matrix.

**Date:**  $t \in R^+$ , Test time.

**Date:**  $\pi_1, \pi_2$ , Horizontal and vertical projection planes.

**Out:**  $[x, y]$ , Cursor position in screen.

```

1. Start
2.   t ← Input_test_time ()
3.   θv ← Input_vertical_angular_range()
4.   θh ← Input_horizontal_angular_range()
5.   xc ← width_screen() / 2
6.   yc ← heigh_screen() / 2

7.   While stop_criterial (), do:
      Calibration process
5.     MAG → mag_calibration_function(XYZ_magnetometer_signal)
6.     ACC → acc_calibration_function(XYZ_accelerometer_signal)
      Low-pass filter
7.     LP-MAG → Low_pass_filter(MAG)
8.     LP-ACC → Low_pass_filter(ACC)
      Get Orientation IMU
9.     H = norm(LP-MAG)
10.    Zs = norm(LP-ACC)
11.    Ys = cross(H, Zs)
12.    Xs = cross(Ys, Zs)
13.    sRs = [Xs, Ys, Zs]3x3
14.    GRS = [GXS, GYS, GZS]3x3 = GR . sRs
      Get position cursor
15.    GXsPπ1 → cross(cross(GXs, ZG), ZG)
16.    GXsPπ2 → cross(cross(GXs, XG), XG)
17.    [Δx, Δy] = [GXsPπ1 (2), GXsPπ2 (3)]
18.    Δx(pixel) = Δx · width_screen() / θh
19.    Δy(pixel) = Δy · heigh_screen() / θv
20.    x = xc + Δx(pixel)
21.    y = yc + Δy(pixel)
22. end

```

Fig. 3. Pseudo-code of the algorithm to translate the angular orientation of the IMU to the pointer positions.

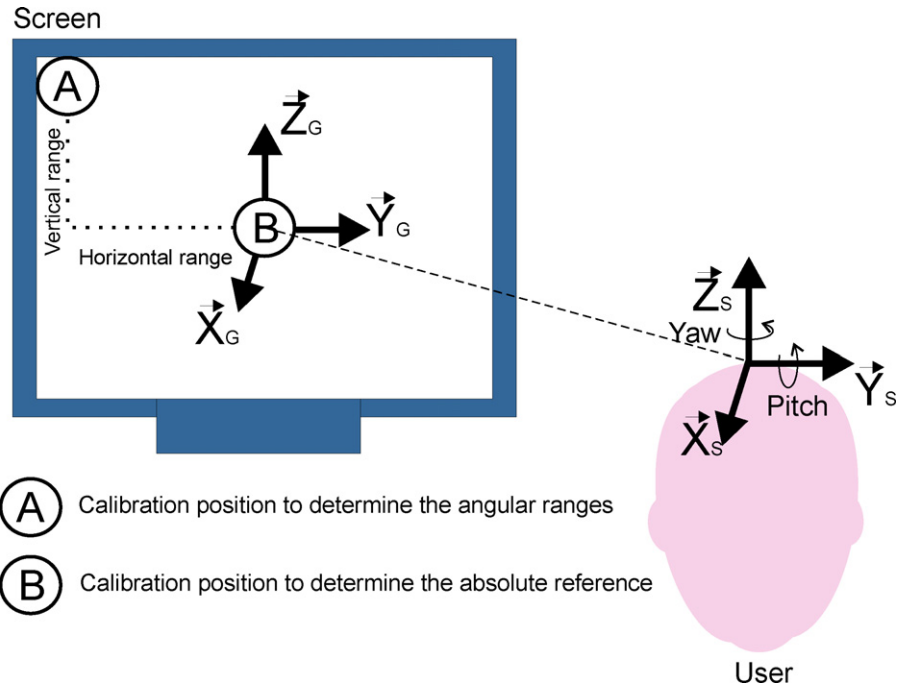


Fig. 4. Steps to calibrate the inertial system using calibration points of the screen A and B. Through points A and B the horizontal and vertical angular ranges are obtained. Looking at the point B, it is obtained the absolute reference frame  ${}^G R$ .

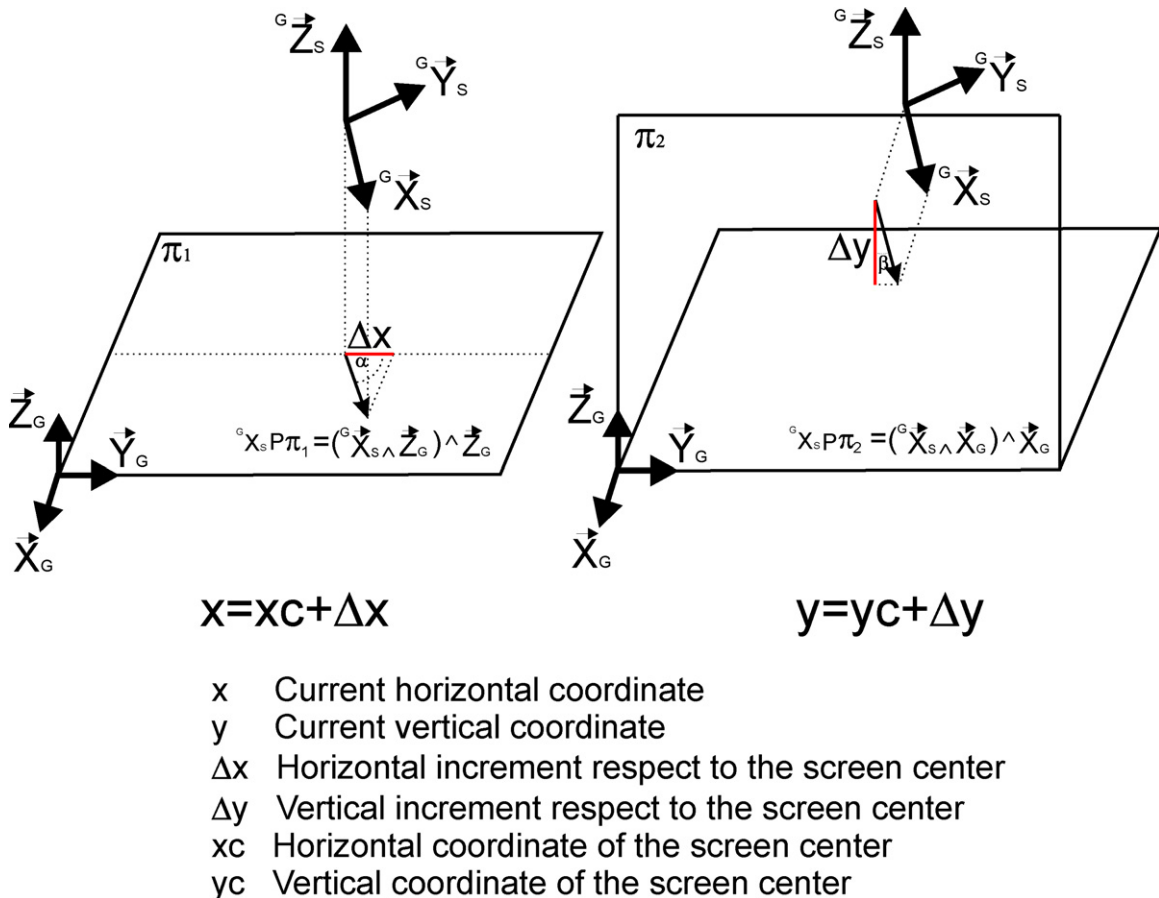


Fig. 5. Correspondence between angular head orientation and pointer coordinates.

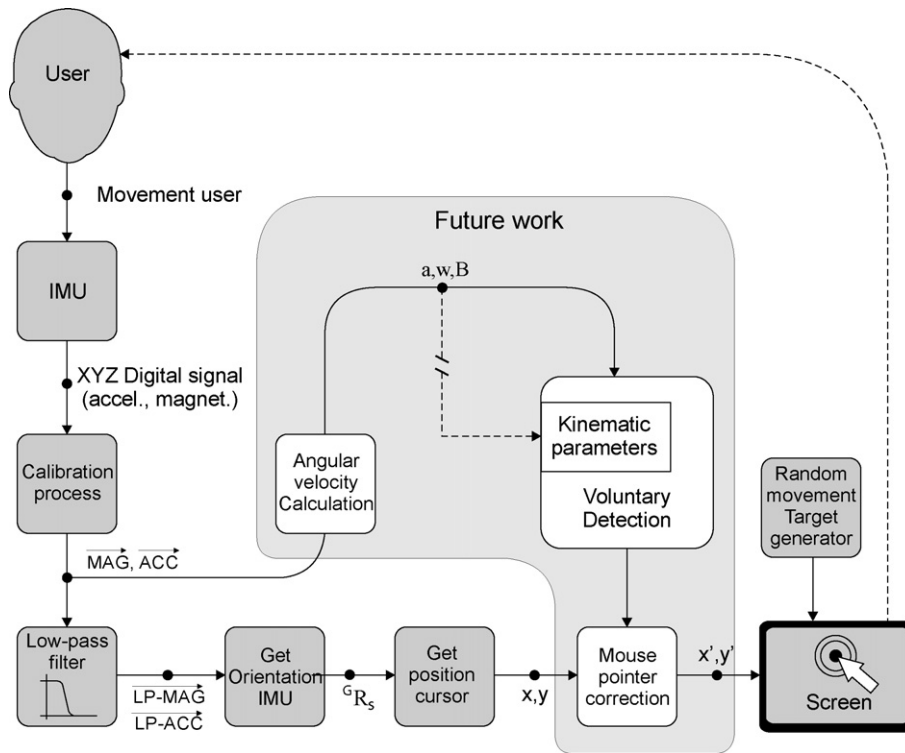


Fig. 6. Block diagram of the inertial interface.

axis  $\vec{Y}_G$  gives the horizontal increment of the pointer ( $\Delta x$ ) respect to the screen center. Hence, the horizontal coordinate of the pointer is calculated by the expression  $x = x_c + \Delta x$ . Similarly, the vector  ${}^G\vec{X}_s$  is projected onto the vertical plane  $\Pi_2$  giving place to the 2D vector called  ${}^G\vec{X}_s \mathbf{P} \Pi_2$ . The geometric projection of this 2D vector on the axis  $\vec{Z}_G$  gives the vertical increment of the pointer ( $\Delta y$ ) respect to the screen center. Hence, the vertical coordinate of the pointer is calculated by the expression  $y = y_c + \Delta y$ . As the units of  $\Delta x$  and  $\Delta y$  must be pixels, a conversion must be carried out according to relation between the angular ranges  $\theta_h$  and  $\theta_v$ , defined by the cali-

bration and the screen resolution (width and height of the screen). Please, see the pseudo-code in Fig. 3, 'Get position cursor'. A block diagram is shown by Fig. 6.

By means of an absolute positioning, the accuracy of the cursor positioning is constant during the whole trial. Other methods with relative positioning showed lack of accuracy during the process. Fig. 7 depicts the correspondence between angular orientation of the IMU and the pointer positions for the following rotations: (a)  $90^\circ$  around  ${}^G\vec{Z}_s$ , at  $t = 1$  s, (b)  $90^\circ$  around  ${}^G\vec{Y}_s$  at  $t = 8$  s and (c)  $90^\circ$  around  ${}^G\vec{X}_s$  at  $t = 17$  s. The corresponding pointer positions are

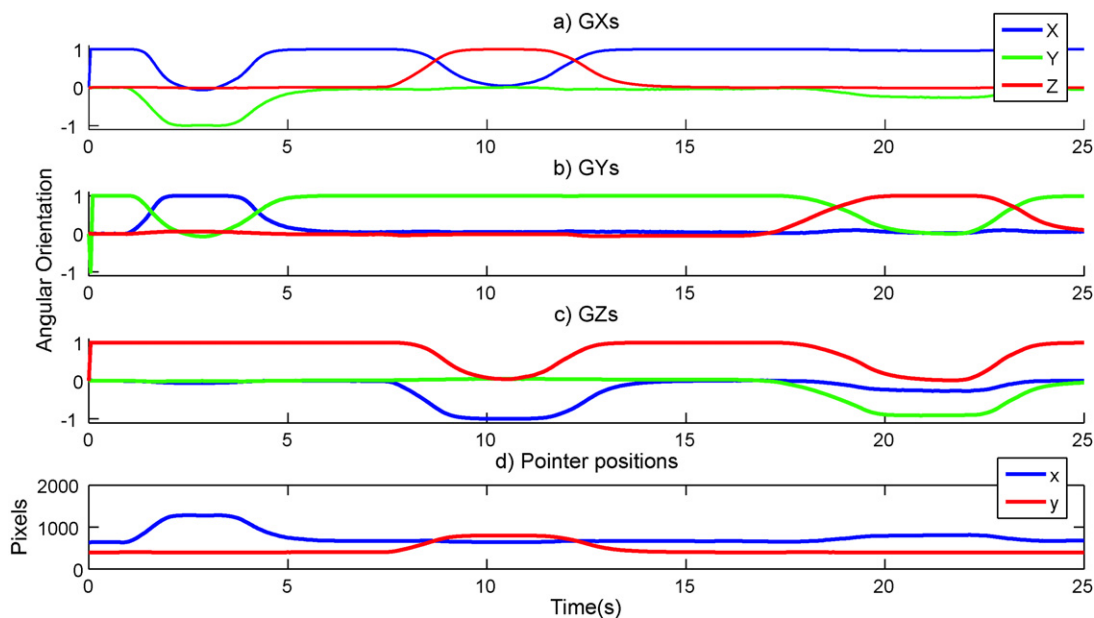


Fig. 7. Absolute orientation and pointer positions versus time. (a–c) Contains the angular orientation of the IMU and (d) contains the horizontal and vertical positions of the pointer.

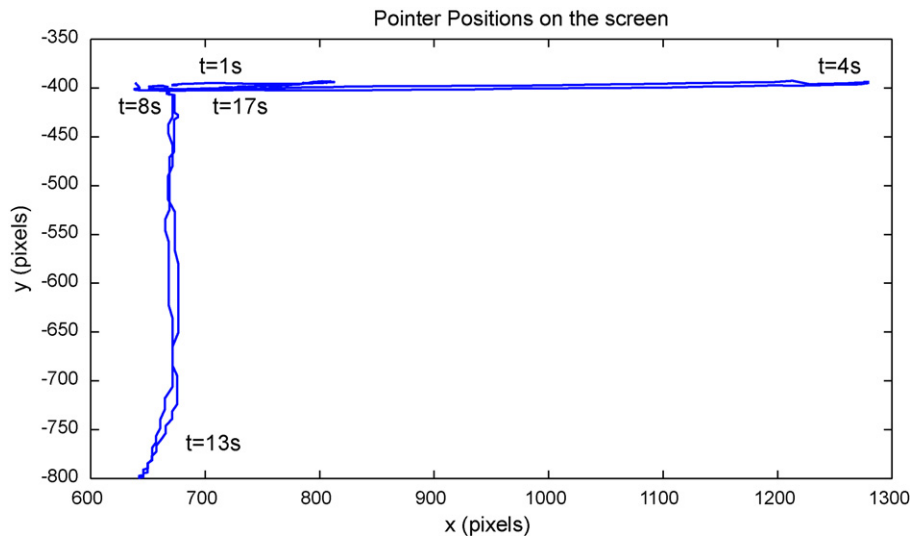


Fig. 8. Pointer positions on the screen.

showed by (d). Both angular ranges were  $90^\circ$  and the screen resolution was  $1280 \times 800$  pixels. The rotation around  ${}^G\bar{Z}_s$  (Yaw motion) causes the pointer moves horizontally (please, note that the red line in (d) does not change). The rotation around  ${}^G\bar{Y}_s$  (Pitch Motion) causes the pointer moves vertically (please, note that the blue line in (d) does not change). The rotation around  ${}^G\bar{X}_s$  (Roll Motion) does not cause any pointer displacement (please, note that both the blue line and the red line in (d) do not change). On one hand, the pointer displacements with rotation around  ${}^G\bar{X}_s$  are undesirable because it generates an unnatural control mode. On the other hand, some infants present drop head because of their muscular diseases, thus producing an involuntary rotation around the cited axis. Hence, these involuntary movements must not have effect on the pointer displacements. Fig. 8 shows the pointer positions on the screen.

### 3.3. Validation of the angular orientation estimation

Some tests were carried out to determine the orientation accuracy. The photogrammetric system BTS SMART-D (High Frequency Digital System for Biomechanical Motion Analysis) was used as absolute reference system. According to the manufacturer technical specifications the system can achieve an accuracy less than 0.2 mm on a volume of  $3\text{ m} \times 2\text{ m} \times 2\text{ m}$ . The trials were carried out with an acquisition frequency of 250 Hz. Four cameras were used on a volume of  $1.75\text{ m} \times 1.30\text{ m} \times 1.8\text{ m}$ . The cameras were oriented to a table where the trials took place (see Fig. 9). They were adjusted for the lighting conditions and the automatic calibration of the BTS

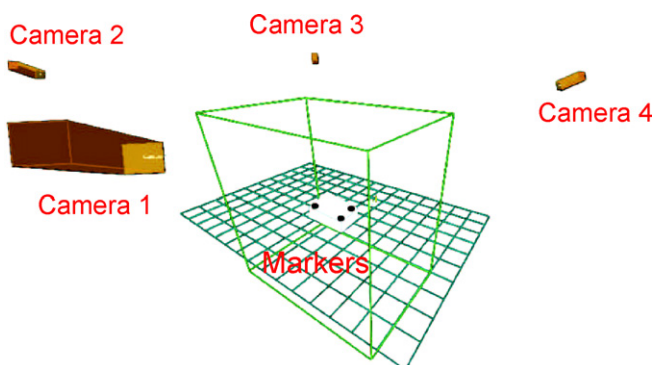


Fig. 9. Setup configuration for the photogrammetric system.

system gave an accuracy which is showed by Table 2. Three markers were placed over the inertial sensor to define the three axes X, Y, Z (Fig. 9). The protocol consisted of a series of gyros around each axis ( $90^\circ$ ). The acquisition frequency of the IMU was 50 Hz. The accuracy and precision assessment of the orientation estimation was carried out by measuring the bias and standard deviation between the inertial sensor and the photogrammetric system. The bias has been defined as the angle between the axis estimated by the inertial sensor and the axis estimated by photogrammetric system. The standard deviation of these angles is calculated to analyze the degree to which repeated measurements show the same results (precision). An example of the comparison of both system is depicted by Fig. 10. The bias and standard deviation have been separately calculated for the static and dynamic period. The mean of the bias of each rotation for the static period was  $1.08^\circ$  and the standard deviation was  $1.20^\circ$ . The mean of the bias of each rotation for the dynamic period was  $1.34^\circ$  and the standard deviation was  $1.38^\circ$ . With errors around  $1^\circ$ , if for example the horizontal angular range is about  $60^\circ$  and the screen resolution is 1024 pixels, the error is about 17 pixels. These conditions are even better if a projector is used instead of the screen of the computer, what not only improves the resolution but also other factors related to the infant, such as attention and motivation.

## 4. Experiments and results

### 4.1. Experiments and results with healthy users

The inertial interface was tested by five healthy users. The ISO 9241-9 standard for computer pointing devices proposes an evaluation performance and comfort [21]. The metric for comparison is Throughput, in bits per second (bits/s), which includes both the

Table 2  
Accuracy of the photogrammetric system.

|                        | Mean  | Std Dev |
|------------------------|-------|---------|
| 3D reconstruction (mm) |       |         |
| Wrand                  | 0.180 | 0.287   |
| 2D residual (pixel)    |       |         |
| Camera 1               | 0.104 | 0.081   |
| Camera 2               | 0.112 | 0.088   |
| Camera 3               | 0.084 | 0.075   |
| Camera 4               | 0.146 | 0.123   |

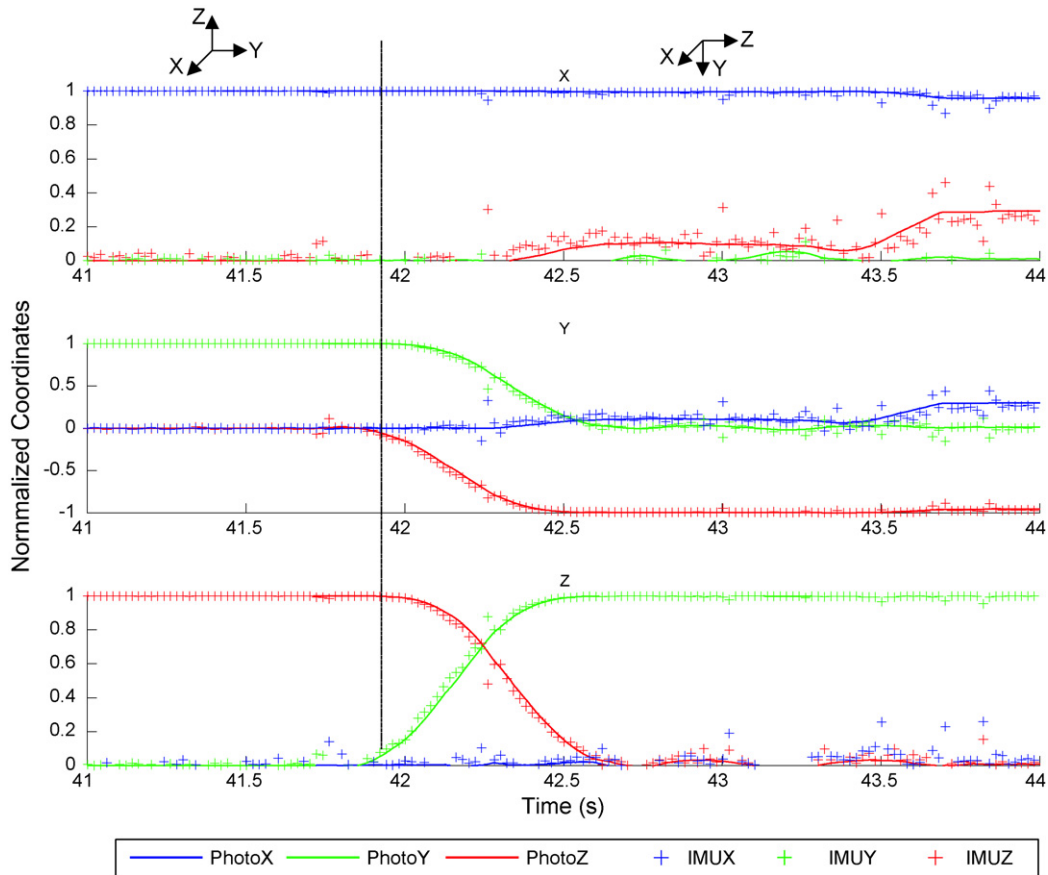


**Fig. 10.** The coordinates X, Y, Z of the absolute orientation for inertial measurement system versus photogrammetric reference corresponding to a rotation of 90° around X axis.

speed and accuracy of users' performance. These tests evaluate the inertial interface in comparison to standard mouse. The equation for throughput is Fitts' Index of Performance except using an effective index of difficulty ( $ID_e$ ). Specifically,

$$Throughput = \frac{ID_e}{MT} \quad (2)$$

where  $MT$  is the mean movement time, in seconds, for all trials within the same condition, and

$$ID_e = \frac{\log_2 D}{W_e + 1} \quad (3)$$

$ID_e$ , in bits, is calculated from  $D$ , the distance to the target, and  $W_e$ , the effective width of the target [27].

Performance testing was limited to reach 16 circular targets which appeared in predefined order around the screen's center. The width of each target was 40 pixels. The sampled frequency of the inertial interface was 20 Hz. The mean of the throughput values with standard deviation for standard mouse and inertial interface is showed by Fig. 11. The throughput parameter was compared to throughput values found in the literature and was found to be in agreement [35,27]. Fig. 12 depicts the coordinates of the pointer and the target versus time for a healthy user. This figure shows the dynamic evolution of the pointer and target coordinates.

The fact that the inertial interface can be used by healthy users, indicates that it might be used by people without head motor limitations. For this reason, the inertial interface will be tested by people with other disabilities as paraplegia.

#### 4.2. Experiments and results with infants with cerebral palsy

Some preliminary experiments involving children were conducted in a CP center called Aspace-Cantabria (Spain). They consisted of moving a cube (simulating the box of the sensor) on the screen according to the infant's head movement. The main goal was to identify the different groups of CP. One of the most important findings was that cerebral palsy is a disorder which involves het-

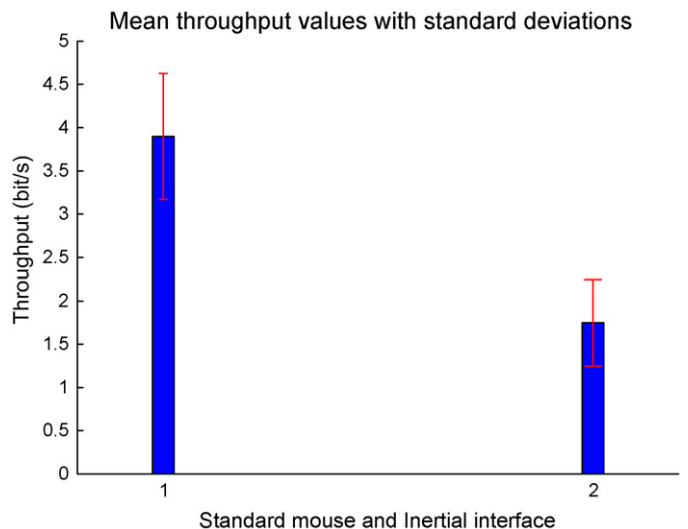


**Fig. 11.** Mean throughput values with standard deviations. Left side: Standard mouse. Right side: Inertial mouse.

**Table 3**  
Clinical characteristics of the subjects with CP.

|      | Functional motor characteristics |              |                      |                       |
|------|----------------------------------|--------------|----------------------|-----------------------|
|      | Cervical tone                    | General tone | Associated movements | Intellectual capacity |
| BCB  | Hypertonia                       | Hypertonia   | Athetosis            | Normal                |
| HGAC | Dystonia                         | Dystonia     | Ballistics           | Normal                |

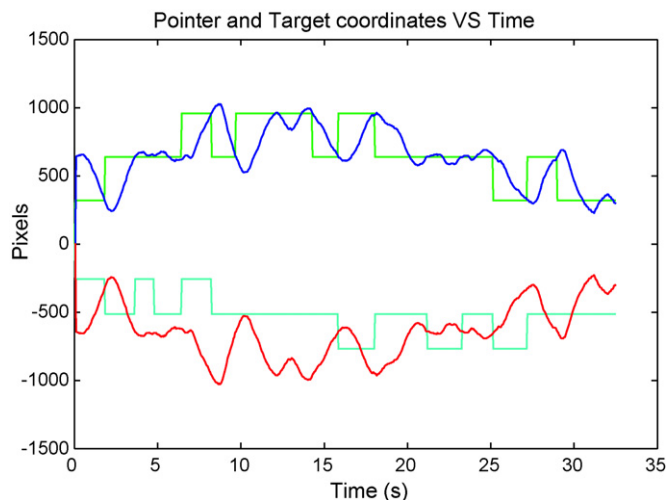


Fig. 12. Pointer and target coordinates for a healthy user.

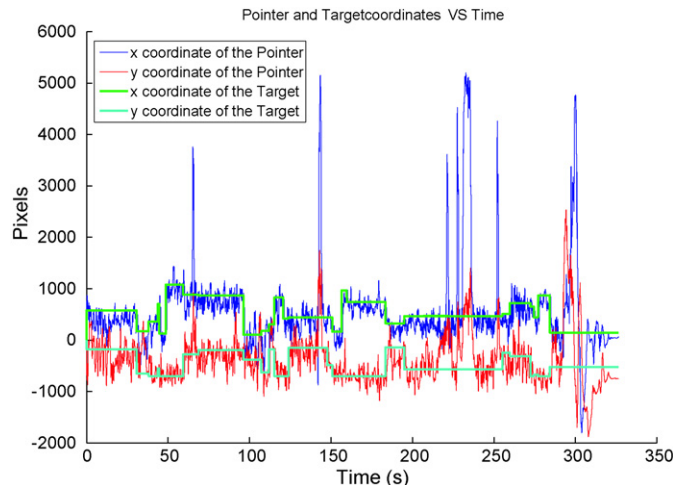


Fig. 13. Pointer and target coordinates versus time for infants with CP without applying filtering techniques.

erogeneous types of motor limitations. Hypotonia for example (low muscle tones) is evidenced by a drooping of the child’s head what makes difficult to control any head-mounted interface. For these cases, it was concluded that a specific solution for this disease is necessary and it will be studied in future researches. For the tests presented by this paper, two children with CP participated, BCB and HGAC. Table 3 collects some clinical patterns of these subjects.

In the tests with infants with CP, a target was randomly placed on a projector and the user had to move his/her head to place the pointer on the center of the target. When the pointer was located over the center of the target, its position was changed. The acquisition frequency was 20 Hz. Fig. 13 depicts the target’s positions and the pointer’s coordinates versus time for the task for BCB without applying filtering techniques. The graphic shows that the involuntary movements are mainly composed of two components, continuous tremorous movements during the whole trial and eventual spasms. However, although involuntary movements appear during the whole trial, the subject can always control the pointer around a region close to the target. It suggests that it may be interesting a control in joystick mode. It means that the pointer could slowly move in one of eight directions (left, right, up, down,

up-right, up-left, down-right, down-left) depending on the current head pose respect to the center of the screen. However, it could result unnatural. Obviously, while a spasm occurs, the control is lost, thus resulting very difficult to resume the control. The results for HGAC were similar, although tremor intensity was less, the ballistic movements caused that the target pointing was slightly more difficult. In order to identify the components involved in the involuntary movements, the spectrogram of the coordinates of the pointer was calculated using the Short-Time Fourier Transform (STFT). The spectrogram shows the power spectral density (PSD) versus time. Fig. 14(a) depicts the spectrogram of the horizontal coordinate of the pointer for HGAC. Red color indicates higher PSD. The continuous tremor has a frequency up to 2 Hz and spasms can reach up to 4–6 Hz. Fig. 14(b) depicts the spectrogram of the horizontal coordinate of the pointer for a healthy user. The spectrogram for a healthy user shows the frequency is between 0 and 1 Hz.

Therefore, these results show that it is necessary to filter the involuntary movements in order to improve the control. The kinematic parameters the IMU offers are interesting to create efficient filtering techniques. The first technique which has been imple-

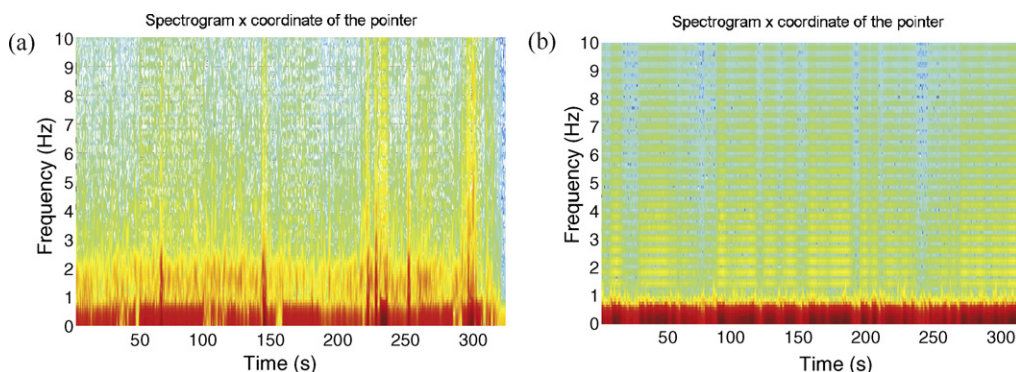


Fig. 14. (a) Spectrogram of the pointer coordinate x for HGAC. (b) Spectrogram of the pointer coordinate x for a healthy user.

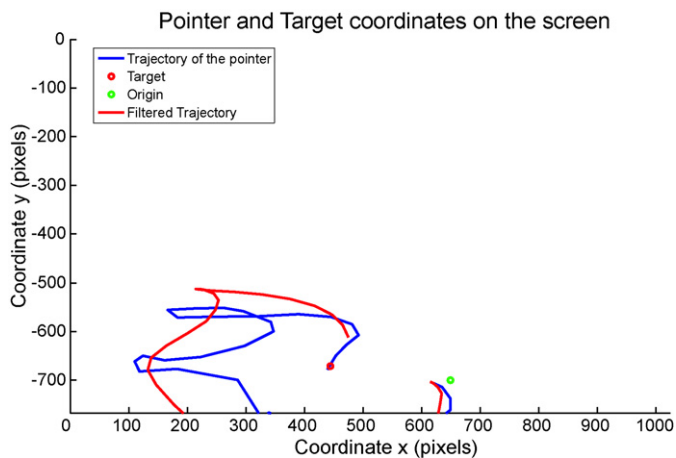


Fig. 15. Trajectory of the pointer from a home point target with and without Benedict Bordner filter performed by BCB.

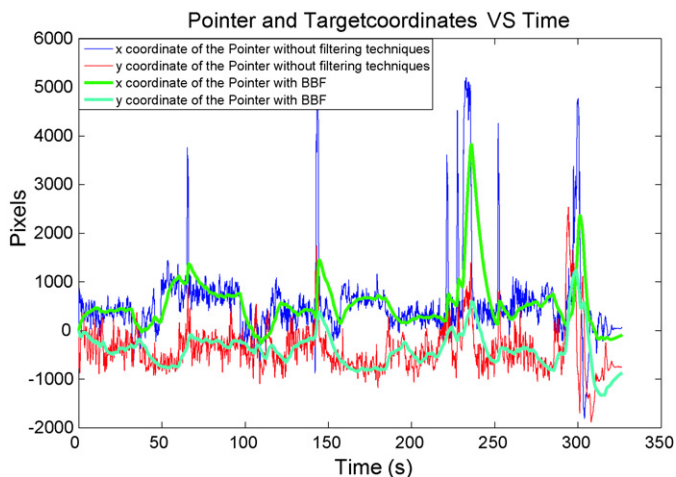


Fig. 16. Pointer and target coordinates versus time for BCB with the Benedict Bordner filter working in real-time.

mented is based on Benedict Bordner filter (BBF) [4]. It is a second order estimator which estimates the future position and speed. Although it is still under researching, it shows interesting results. Fig. 15 shows the trajectory of the pointer (blue line) from a origin point (green) to a target point (red). Notice that the trajectory is not as straight as possible. By using the BBF filter a straighter trajectory (red line) is obtained. Fig. 16 shows the results of filtering the cursor coordinates of the tests showed in Fig. 13. Notice that the undesirable movements are filtered improving the control of the pointer.

## 5. Conclusions and future work

The alternative interface presented by this paper aims to design a mouse replacement for infants with CP. This research arises from the fact that their motor disabilities make difficult to access to the computer, thus diminishing the opportunities to communicate or learn through the computer. Although, there are a wide variety of advanced interfaces for disabled people, few researches are focused on controlling the interface with pathological movements, filtering the involuntary motion and detecting the intentions. Therefore, for these types of interfaces, a characterization of the pathological motion is required. The inertial technology has been preferred over others because inertial sensors offer kinematic parameters (accel-

erations, angular velocity, etc.) directly without needing complex algorithms.

According to the tests performed by healthy users, the inertial interface results usable as stated by the metrics described by the standard ISO 9241. For this reason, in the future, the inertial interface will be tested by disabled people whose upper limb capabilities are constrained, but have normal capabilities of their head. The tests performed by infants with CP, show that although they can locate the pointer around the target, they have limitations when a fine motor control is required. As the results show, the inertial interface shows interesting information about the pathological movement what results very useful to design the filtering techniques to detect the user's intentions. A researching technique is presented by this paper. It offers promising preliminary results.

The clinical professional of Aspace-Cantabria evaluated the interface as an useful tool for communicating, learning and therapy. The inertial interface provides the feedback of the users' movements what helps them to improve their proprioception and the normalization of their movements. The inertial interface can be used to control some assistive softwares, such as virtual keyboards, video-games or multimedia applications to improve the communication with the environment both physical and social. The IMU results comfortable for wearable interfaces because only a small and lightweight device is necessary. The calibration process has been minimized so that the clinical professional can do it (defining the angular ranges at the beginning of the use), without requiring a tedious process for the infant.

From the technical point of view, this paper presented a real-time algorithm to estimate the angular orientation of the IMU with an accuracy about  $1^\circ$ . The algorithm to translate the angular orientation to pointer locations is designed so that the rotation around the axis perpendicular to the screen ( $X$ ) does not produce pointer displacements because many infants incline involuntarily their head around the cited axis and the effects of this movements have been cancelled. This algorithm uses an absolute positioning of the pointer what ensures the accuracy is kept constant during the use.

In the next future, some filtering techniques will be designed and evaluated with infants with CP. The intended inertial interface will detect the patterns of infants with different types of involuntary movements and detect the intentions to improve the control of the pointing device. A characterization of the pathological movements will be carried out in terms of kinematic parameters. The different filters and settings for each group of infants with CP will be identified. Moreover, the potential of the inertial interface as rehabilitation tool will be analyzed. Some softwares will be designed to provide a real-time feedback of the users' motion, what will be useful to know the learning progress and the success of the therapy.

## Acknowledgments

The authors would like to express their gratitude to Aspace-Cantabria for its fundamental collaboration and the investment of the project ENLAZA by IMSERSO (Spain).

## References

- [1] J. Bache, G. Derwent, Access to computer-based leisure for individuals with profound disabilities, *NeuroRehabilitation* 23 (2008) 343–350.
- [2] R. Bates, H.O. Istance, Why are eyemice unpopular? a detailed comparison of head and eye controlled assistive technology pointing devices, *Universal Access in the Information Society* 2 (2003) 280–290.
- [3] M.C. Bax, Terminology and classification of cerebral palsy, *Developmental Medicine and Child Neurology* 6 (1964) 295–297.
- [4] T.R. Benedict, G.W. Bordner, Synthesis of an optimal set of radar track-while scan smoothing equations, *IRE Transactions on Automatic Control* 7 (4) (1962) 27–32.

- [5] M. Betke, J. Gips, P. Fleming, The camera mouse: visual tracking of body features to provide computer access for people with severe disabilities, *IEEE Transactions on Neural Systems and Rehabilitation Engineering* 10 (1) (2002) 1–10.
- [6] M. Betke, Intelligent interfaces to empower people with disabilities, in: *Handbook of Ambient Intelligence and Smart Environments*, 2010, pp. 409–432, ISBN: 978-0-387-93807-3.
- [7] J.A. Birmes, X. Li, J. Malkin, K. Kilanski, R. Wright, K. Kirchoff, A. Subramanya, S. Harada, J.A. Landay, P. Dowden, H. Chizeck, The vocal joystick: a voice-based human–computer interface for individuals with motor impairments, in: *Proceedings of the Conference on Human Language Technology and Empirical Methods in Natural Language Processing*, 2005.
- [8] M. Böhme, M. Haker, T. Martinetz, E. Barth, A facial feature tracker for human–computer interaction based on 3d of cameras, in: *Dynamic 3D Imaging—Workshop in Conjunction with DAGM*, 2008.
- [9] P. Bonnat, Method and system for controlling a user interface of a device using human breath, Technical Report, Patent No. US 2008/0177404 (2008).
- [10] R. Ceres, J.L. Pons, L. Calderón, A.R. Jiménez, L. Azevedo, Palma, a robotic vehicle for assisted mobility of disabled children, *IEEE Engineering in Medicine and Biology Magazine* 24 (6) (2005) 55–63.
- [11] Y.-L. Chen, Application of tilt sensors in human–computer mouse interface for people with disabilities, *IEEE Transactions on Neural Systems and Rehabilitation Engineering* 9 (3) (2001) 289–294.
- [12] C.A. Chin, A. Barreto, J.G. Cremades, M. Adjouadi, Integrated electromyogram and eye-gaze tracking cursor control system for computer users with motor disabilities, *Journal of Rehabilitation Research & Development* 45 (1) (2008) 161–174.
- [13] C. Conno, E. Yu, J. Magee, E. Cansizoglu, S. Epstein, M. Betke, Movement and recovery analysis of a mouse-replacement interface for users with severe disabilities in universal access in human–computer interaction, in: *Intelligent and Ubiquitous Interaction Environments*, 2009, pp. 493–502, ISBN: 978-3-642-02709-3.
- [14] F.X. DiMattia, P. Curran, J. Gips, An Eye Control Teaching Device for Students Without Language Expressive Capacity: EagleEyes, Edwin Mellen, Lampeter, U.K., 2001.
- [15] G.-M. Eom, K.-S. Kim, C.-S. Kim, J. Lee, S.-C. Chung, B. Lee, H. Higa, N. Furuse, R. Futami, T. Watanabe, Gyro-mouse for the disabled: 'click' and 'position' control of the mouse cursor, *International Journal of Control, Automation, and Systems* 5 (2) (2007) 147–154.
- [16] D.G. Evans, R. Drew, P. Blenkhorn, Controlling mouse pointer position using an infrared head-operated joystick, *IEEE Transactions on Rehabilitation Engineering* 8 (1) (2000) 107–117.
- [17] F. Ferraris, U. Grimaldi, M. Parvis, Procedure for effortless in-field calibration of three-axis rate gyros and accelerometers, *Sensors and Materials* 7 (5) (1995) 311–330.
- [18] A. Gesell, *The First Five Years of Life*, Methuen, 1966.
- [19] S. Harada, J.O. Wobbrock, J. Malkin, J.A. Birmes, J.A. Landay, Longitudinal study of people learning to use continuous voice-based cursor control, in: *Proceedings of the 27th International Conference on Human Factors in Computing Systems*, 2009, pp. 347–356.
- [20] F.C. Hummel, L.G. Cohen, Drivers of brain plasticity, *Current Opinion in Neurology* 18 (2005) 667–674.
- [21] International Organization for Standardization International Standard, Ergonomic requirements for office work with visual display terminals (vds). Part 9. Requirements for non-keyboard input devices, Technical Report, ISO/DIS 9241-9, 2000.
- [22] A. Johnson, Prevalence and characteristics of children with cerebral palsy in Europe, *Developmental Medicine and Child Neurology* 44 (9) (2002) 633.
- [23] M.A. Jones, I. McEwen, L. Hansen, Use of power mobility for a young child with spinal muscular atrophy, *Physical Therapy* 83 (3) (2003) 253–262.
- [24] M. Ketelaar, A. Verneer, H. Hart, E. van Petergern Beek, P. Helder, Effects of a functional therapy program on motor abilities of children with cerebral palsy, *Physical Therapy* 81 (9) (2001) 1534–1545.
- [25] E.F. LoPresti, A. Mihailescu, N. Kirsch, Assistive technology for cognitive rehabilitation: state of the art, *Neuropsychological Rehabilitation* 14 (1/2) (2004) 5–39.
- [26] H.J. Luinge, P.H. Veltink, Measuring orientation of human body segments using miniature gyroscopes and accelerometers, *Medical & Biological Engineering & Computing* 43 (2005) 273–282.
- [27] I.S. MacKenzie, Fitts' law as a research and design tool in human–computer interaction, *Human–Computer Interaction* 7 (1992) 91–139.
- [28] M. Malka, A. Weise, S. Shulman, The facilitation of information processing in learning disabled children using computer games, *Physical Therapy* 7 (1) (1987) 47–54.
- [29] K.A. Mann, F.W. Werner, A.K. Palmer, Frequency spectrum analysis of wrist motion for activities of daily living, *Journal of Orthopedic Research* 7 (2) (1989) 304–306.
- [30] C. Manresa-Yee, J. Varona, T. Ribot, F.J. Perales, Non-verbal communication by means of head tracking, in: *Ibero-American Symposium on Computer Graphics—SIACG*, 2006.
- [31] D.W.K. Man, M.S.L. Wong, Evaluation of computer-access solutions for students with quadriplegic athetoid cerebral palsy, *American Journal of Occupational Therapy* 61 (2007) 355–364.
- [32] C. Mauri, T. Granollers, J. Lorés, M. García, Computer vision interaction for people with severe movement restrictions, *An Interdisciplinary Journal on Humans in ICT Environments* 2 (1) (2006) 38–54.
- [33] M. Mazo, J.C. García, F.J. Rodríguez, J. Ureña, J.L. Lázaro, F. Espinosa, the SIAMO research team, Experiences in assisted mobility: the siamo project, in: *Proceedings of the 2002 IEEE International Conference on Control Applications*, 2002.
- [34] MT9, [www.xsens.com/en/general/mti](http://www.xsens.com/en/general/mti).
- [35] J. Music, M. Cecic, M. Bonkovic, Testing inertial sensor performance as hands-free human–computer interface, in: *Wseas Transactions on Computers*, 2009.
- [36] W. Nutt, C. Arlanck, S. Nigg, G. Staufert, Tongue-mouse for quadriplegics, *Journal of Micromechanics Microengineering* 8 (1998) 155–157.
- [37] World Health Organization, Disability and rehabilitation who action plan 2006–2011, Technical Report, 2006, [www.who.int/disabilities/publications](http://www.who.int/disabilities/publications).
- [38] G. Pfurtscheller, B. Graimann, C. Neuper, Eeg-based brain–computer interface systems and signal processing, *Encyclopedia of Biomedical Engineering*, Wiley and Sons 2 (2006) 1156–1166.
- [39] G. Pfurtscheller, C. Neuper, N. Birbaumer, Human brain–computer interface in motor cortex in voluntary movements, *CRS Press*, 2005, pp. 367–401.
- [40] J.L. Pons, R. Ceres, E. Rocon, S. Levin, I. Markovitz, B. Saro, D. Reynaerts, D. Van Moorleghem, L. Bueno, Virtual reality training and emg control of the manus hand prosthesis, *Robotica* 23 (2005) 311–317.
- [41] R. Poppe, Vision-based human motion analysis: an overview, *Computer Vision and Image Understanding* 108 (2007) 4–18.
- [42] L. Qian, W.-y. Chen, G.-p. Xu, Application of novel rotation angular model for 3d mouse system based on mems accelerometers, *Journal of Shanghai Jiaotong University (Science)* 14 (2) (2009) 137–142.
- [43] D.M. Riby, P.J.B. Hancock, Do faces capture the attention of individuals with williams syndrome or autism? evidence from tracking eye movements, *Journal of Autism and Developmental Disorders* 39 (3) (2009) 421–431.
- [44] E. Rocon, J.C. Moreno, A.F. Ruiz, F. Brunetti, J.A. Miranda, J.L. Pons, Application of inertial sensors in rehabilitation robotics, in: *Proceedings of the 2007 IEEE 10th International Conference on Rehabilitation Robotics*, 2007.
- [45] E. Rocon, A. Ruiz, J.L. Pons, On the use of rate gyroscopes for tremor sensing in the human upper limb, in: *Of the International Conference EuroSensors XIX*, 2005.
- [46] D. Roetenberg, H.J. Luinge, C.T.M. Baten, P.H. Veltink, Compensation of magnetic disturbances improves inertial and magnetic sensing of human body segment orientation, *IEEE Transactions on Neural Systems and Rehabilitation Engineering* 13 (3) (2005) 395–405.
- [47] Y. Swinth, D. Anson, J. Deitz, Single-switch computer access for infants and toddlers, *The American Journal of Occupational Therapy* 47 (11) (1993) 1031–1038.
- [48] Y. Tao, H. Hu, H. Zhou, Integration of vision and inertial sensors for 3d arm motion tracking in home-based rehabilitation, *The International Journal of Robotics Research* 26 (6) (2007) 607–624.
- [49] J.L. Tu, T. Huang, H. Tao, Face as mouse through visual face tracking, in: *IEEE CRV'05*, 2005, pp. 339–346.
- [50] M. Wichers, S. Hilberink, M. Roebroek, O.V. Nieuwenhuizen, H. Stam, Motor impairments and activity limitations in children with spastic cerebral palsy: a Dutch population-based study, *Journal of Rehabilitation Medicine* 41 (5) (2009) 367–374 (8).
- [51] S. Winter, A. Autry, M. Yeargin-Allsopp, Trends in the prevalence of cerebral palsy in a population-based study, *Pediatric* 110 (6) (2002) 1220–1225.
- [52] C.E.B. Vilvestad, N.K. Stensj, The use and impact of assistive devices and other environmental modifications on everyday activities and care in young children with cerebral palsy, *Disability and Rehabilitation* 27 (14) (2005) 849–861.

## Biographies

**Rafael Raya** graduated in electronic and automatic engineering from Universidad de Córdoba, Spain, in 2006. Since 2006, he is with Spanish National Council for Science Research (CSIC) and he has been working in the bioengineering group. Since 2007, he is also a Ph.D. student at the Universidad de Alcalá, Spain. He has participated in different national and international scientific projects and congresses developing different publications. His research interests include rehabilitation robotics, biomechanics, and human machine interaction.

**Javier O. Roa** was born in Colombia, in 1975. He received the technical electronic engineer degree from the Unidades Tecnológicas de Santander, Bucaramanga, Colombia, in 1996 and the degree in electronic engineering from the Universidad del Valle, Cali, Colombia, in 2003. He is currently working toward the PhD degree in electronics with the Universidad de Alcalá, Madrid, Spain. Since 2004, he has been a researcher with the Instituto de Automática Industrial, Consejo Superior de Investigaciones Científicas (CSIC), Madrid. His current research interests are in the field of optimization methods using metaheuristic techniques and concepts of artificial intelligence, such as evolutionary algorithms, fuzzy logic, and artificial neural networks.

**Dr. Eduardo Rocon** is with CSIC since 2001. He is currently research assistant at CSIC. His research interests include rehabilitation robotics, biomechanics, adaptive signal processing, and human machine interaction. His main field of expertise is in active control of human–machine interaction, and the main topic of his doctoral dissertation was active tremor suppression through exoskeleton-based application of load.

**Dr. Ramón Ceres** graduated in physics (electronics) from Universidad Complutense de Madrid, Spain, in 1971 and received the PhD degree in 1978. Following a year

the laboratoire d'Analyse et d'Architecture des Systèmes Centre National de la Recherche Scientifique (LAAS CNRS) in Toulouse, France, he has been working at the Instituto de Automatica Industrial (IAI), a division of the Spanish National Council for Science Research (CSIC), as center head of the systems department and deputy director. He was research and development director of AUTELEC, a company working in the electronic field, the Spanish delegate of the regulatory committee of the BRITE/EURAM Program, and general coordinator of the Innovation Projects IBEROEKA within the Iberoamerican research and development program CYTED. At present, he is a professor of research at the CSIC. He has received several awards, including the International Award of the ONCE. He has managed more than 60 national and international projects with more of 140 papers.

**Dr. José L. Pons** received a BS degree in mechanical engineering from the Universidad de Navarra Engineering in 1992, the MS degree in 1994 from Universidad Politecnica de Madrid, and a PhD degree in 1996 from the Universidad Complutense de Madrid. He is with the IAI-CSIC since 1993 and has actively participated in a number of National, European and International RTD projects in the area of microsystem technologies and advanced sensors, actuators and control. In particular, he is co-ordinating the GAIT project (IST-2001-37751) and the Spanish consortium within the Eureka PAMIS project devoted to production technologies for custom-made microsensors. In addition he has been the technical and administrative co-ordinator of several national and European projects. In particular it is worth mentioning his work on control of advanced microactuators in the framework of projects DRIFTS, ACTUA and MUS, as well as in MANUS (TELEMATICS).